이학석사학위논문

이리듐 복합체를 이용한 전기화학적 발광 기반의 황화이온 프로브

Electrogenerated Chemiluminescent Probes for Sulfide Based on Cyclometalated Ir(III) Complexes

2017 년 2 월

서울대학교 대학원

화학부 유기화학전공

김 서 연

Electrogenerated Chemiluminescent Probes for Sulfide Based on Cyclometalated Ir(III) Complexes

by

Seo-Yeon Kim

Supervisor: Prof. Jong-In Hong

A Thesis for the Master Degree

In Organic Chemistry

Department of Chemistry

Graduate School

Seoul National University

Abstract

Electrogenerated Chemiluminescent Probes for Sulfide Based on Cyclometalated Ir(III) Complexes

Seo-Yeon Kim

Major in Organic Chemistry

Department of Chemistry

Graduate School

Seoul National University

A variety of chemosensors have been developed for the detection of H_2S. However, most conventional methods require bulky equipment and complicated operations during their anlaysis processes, preventing their use for simple detections for clinical applications.

Electrogenerated chemluminsecnece (ECL)-based chemosensors provide several advantages over existing analytical techniques, including no background signal, high sensitivity, and cost-and time-efficient analysis with simple sensing tools. These features enable ECL systems to be powerful candidates for point-of-care (POC) detection tools.

In this study, we designed and synthesized two ECL chemosensors (**1**, **2**) for sulfide anion based on Ir(III) complexes. The dinitrophenyl (DNP) group was introduced to the Ir(III) complex as a photo-induced electron transfer (PET) quencher as well as a reaction site with sulfide. In the presence of sulfide, the DNP group was cleaved through nucleophilic aromatic substitution (S_NAr), inducing a great enhancement of phosphorescence and ECL. Probe **1** and **2** increased the ECL signals with a linear correlation in the range of 0 to 8 equiv of sulfide, and the limit of detection (LOD) was calculated to be a low value in both cases. In addition, probe **1** and **2** exhibited highly selective ECL responses toward sulfide over various anions and biothiols.

Keywords: Electrogenerated chemiluminescence (ECL), Cyclometalated Ir(III) complex, Chemosensor, Chemodosimeter, Photo-induced electron transfer (PET), Sulfide.

Student number: 2015-20373

Contents

A. Background

B. Electrogenerated Chemiluminescence Probes for Sulfide Based on Cyclometalated Ir(III) Complexes

A. Background

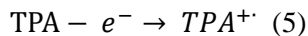## A.1 The Fundamentals of ECL analysis

Electrogenerated Chemiluminescence (ECL) refers to a light-emitting process caused by the electron-transfer reaction between electrochemically generated radical species at the electrodes.[1] ECL luminophores such as $Ru(bpy)_3^{2+}$, Ir(III) complexes, and quantum dot generate light emission at the electrode with a voltage application.

The ECL method differs from conventional analytical methods because ECL requires no extra light sources, allowing simple and miniaturized detection devices.[1, 2] Moreover, the electrochemical approach allows control of the time and positions of light emission and provides high sensitivity, a wide linear detection range, and no background signals. For these reasons, ECL-based assays have been used for the detection of biomolecules in food and water,[3, 4] and have been applied to detect various clinically important analytes with high sensitivity.[1]

The early ECL studies originated with annihilation.[5, 6] This method involves electron-transfer reactions between electrochemically generated species at the working electrode by the alternate pulsing of the potential. Emission is possible if the ECL emitter (A) produces sufficiently stable radical ions, including both an oxidized ($A^{+\cdot}$) and a reduced ($A^{-\cdot}$) form of the emitting molecules in electrochemical condition. The general mechanism of annihilation is outlined below.

$$A + e^- \rightarrow A^{-\cdot} \text{ (Reduction at electrode) (1)}$$

$$A - e^- \rightarrow A^{+\cdot} \text{ (Oxidation at electrode) (2)}$$

$$A^{-\cdot} + A^{+\cdot} \rightarrow A^* + A \text{ (Excited state formation by annihilation) (3)}$$

$$A^* \rightarrow A + h\nu \text{ (Light emission) (4)}$$

In addition to annilhilation ECL, it is also possible to generate ECL with one directional potential scanning at an electrode in a solution containing luminophore species and coreactant.[7-9] A coreactant is a compound that produces a strong reducing or oxidizing agent that can produce excited states of ECL luminophores through an electrochemical electron transfer reaction. Thus far, tri-n-propylamine (TPA) is the most efficient coreactant for oxidative reduction ECL process.[10] There is a commercially important example using TPA as a coreactant involving the Ru(bpy)$_3$$^{2+}$/TPA system.[10] Upon oxidation, TPA initially produces a short-lived TPA radical cation (TPA$^+$), which rapidly deprotonates to form a strongly reducing radical species TPA$^{\cdot}$.[11]

$$TPA - e^- \rightarrow TPA^{+\cdot} \text{ (5)}$$

$$TPA^{+\cdot} \rightarrow TPA^{\cdot} + H^+ \text{ (6)}$$

The proposed ECL generating mechanisms of Ru(bpy)$_3$$^{2+}$/TPA systems are shown in Figure 1.[10] These principles can be extended to ECL systems that use other metal complexes as a luminophore or alternative aliphatic amines as a coreactant.
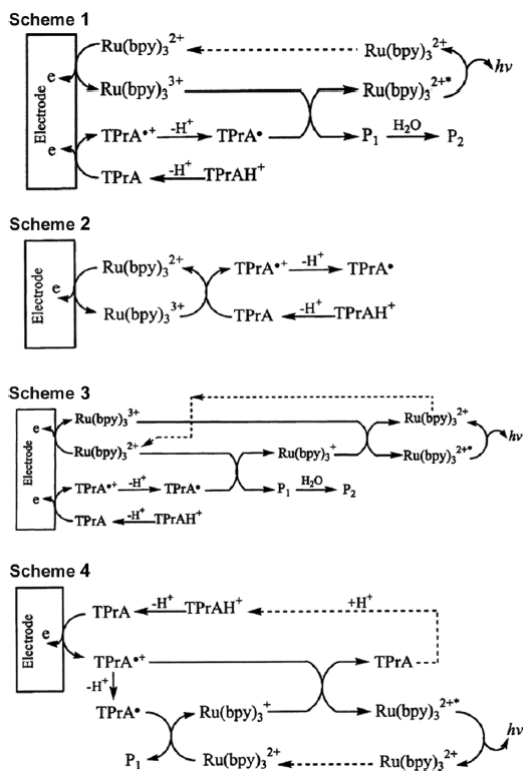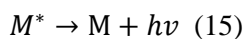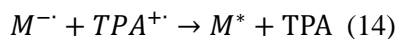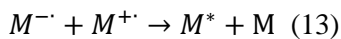
Scheme 1

Electrode

Ru(bpy)$_3$$^{2+}$ ← - - - - - - - Ru(bpy)$_3$$^{2+}$ ↘ hv

Ru(bpy)$_3$$^{3+}$ —————→ Ru(bpy)$_3$$^{2+*}$

TPrA$^{•+}$ —$^{-H^+}$→ TPrA$^{•}$ ——→ P$_1$ —^{H_2O}→ P$_2$

TPrA ←$^{-H^+}$— TPrAH$^+$

Scheme 2

Electrode

Ru(bpy)$_3$$^{2+}$ ← TPrA$^{•+}$ —$^{-H^+}$→ TPrA$^{•}$

Ru(bpy)$_3$$^{3+}$ → TPrA ←$^{-H^+}$— TPrAH$^+$

Scheme 3

Electrode

Ru(bpy)$_3$$^{3+}$

Ru(bpy)$_3$$^{2+}$ ——→ Ru(bpy)$_3$$^{+}$ → Ru(bpy)$_3$$^{2+}$ ↘ hv

Ru(bpy)$_3$$^{2+*}$

TPrA$^{•+}$ —$^{-H^+}$→ TPrA$^{•}$ ——→ P$_1$ —^{H_2O}→ P$_2$

TPrA ←$^{-H^+}$— TPrAH$^+$

Scheme 4

Electrode

TPrA ←$^{-H^+}$— TPrAH$^+$ ← - - - - - $^{+H^+}$ - - -

TPrA$^{•+}$ ——————→ TPrA - - -

-H$^+$ ↓

TPrA$^{•}$ → Ru(bpy)$_3$$^{+}$ ——→ Ru(bpy)$_3$$^{2+*}$ ↘ hv

P$_1$ ← Ru(bpy)$_3$$^{2+}$ ← - - - - - Ru(bpy)$_3$$^{2+}$

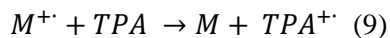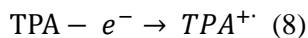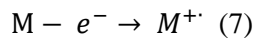**Figure 1** The mechanisms of coreactant ECL for Ru(bpy)$_3$$^{2+}$/TPA system

The key reaction steps for general coreactant ECL systems with TPA is as follows. M represents emitter species.

$$\mathrm{M} - e^- \rightarrow M^{+•} \quad (7)$$

$$\mathrm{TPA} - e^- \rightarrow TPA^{+•} \quad (8)$$

$$M^{+•} + TPA \rightarrow M + TPA^{+•} \quad (9)$$

$$TPA^{+•} \rightarrow TPA^{•} + H^+ \quad (10)$$

$$M^{+•} + TPA^{•} \rightarrow M^* + side\ product \quad (11)$$

$$M + TPA^{•} \rightarrow M^{-•} + side\ product \quad (12)$$

$$M^{-•} + M^{+•} \rightarrow M^* + \mathrm{M} \quad (13)$$

$$M^{-•} + TPA^{+•} \rightarrow M^* + \mathrm{TPA} \quad (14)$$

$$M^* \rightarrow \mathrm{M} + hv \quad (15)$$

3
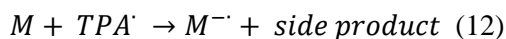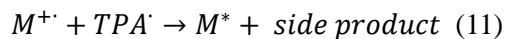
A.2 ECL luminophores

In the past several years, a large number of electrogenerated luminescent species have been developed and their luminescence properties investigated. The studies aimed to find new ECL emitters with electrochemical stability and high ECL efficiency. Luminophores have also been studied for bio-applications by modifying a moiety of the luminophores in various ways.

The organic ECL luminophores were developed in the early stage of the studies, involving polycyclic aromatic hydrocarbons (PAHs) such as anthracene and rubrene.[12] The ECL emission of PAHs were generated in aprotic media through either the annihilation or coreactants method. However, PAHs are limited for practical application due to their poor solubility and the requirement of an additional purification procedure. Non-PAHs, including perylene diimide,[13] fluorescein and BODIPY (boron dipyrromethene)[14] have also been studied. Specifically, completely substituted BODIPY dyes are considerably stable in electrochemical conditions; they induce quite intense ECL emissions by both annihilation and oxidative-reduction coreactant mechanisms.
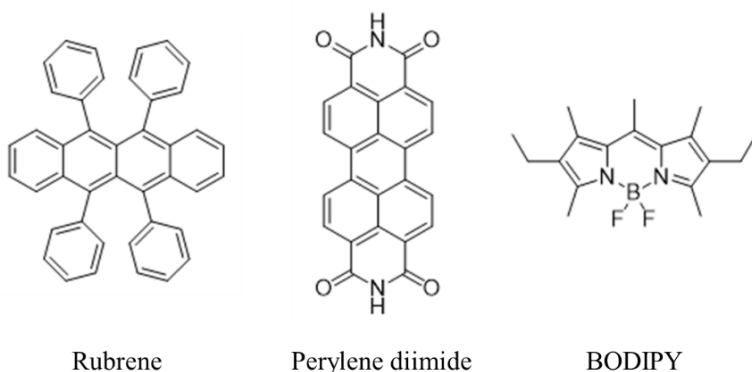

Rubrene   Perylene diimide   BODIPY

Figure 2 ECL-active luminophores (organic systems)

Inorganic systems containing Ag, Al, Au, Cd, Cr, Cu, Eu, Hg, Ir, Mo, W, Os, Pd, Pt, Re, Ru, Si, Tb, and Tl, have been studied for ECL luminophores due to their excellent photophysical properties and electrochemical stability. Among them, the first report of an inorganic complex ECL involved $Ru(bpy)_3^{2+}$, which shows high luminescence, good solubility in various solvents and reversible electron transfer at mild potentials. For example, Bard group discovered that the ECL efficiency of $Ru(bpy)_3^{2+}$ is 0.0500 and that an emitting excited state can be realized with nearly 100% efficiency via an annihilation reaction.[15] The ECL of $Ru(bpy)_3^{2+}$ with coreactant such as oxalate ion $(C_2O_4^{2-})$,[16] peroxydisulfate $(S_2O_8^{2-})$[17] and tri-n-propylamine (TPA)[18] was also studied.

In particular, cyclometalated Ir(III) complexes have been widely studied for ECL lumiophores due to their high ECL efficiencies and easy tunability of emission color by a ligand modification approach. Although the initial study of $Ir(ppy)_3$ ECL showed low intensity via annihilation, there have been many efforts to improve the ECL performance of the Ir(III) complex, starting with the oxidative-reduction ECL study by Richter, M. M. et al.[19] Since then, several red-emitting Ir(III) complexes, such as $(pq)_2Ir(tmd)$, $(pq)_2Ir(acac)$, and $(piq)_2Ir(acac)$, have been reported, showing higher ECL efficiencies than
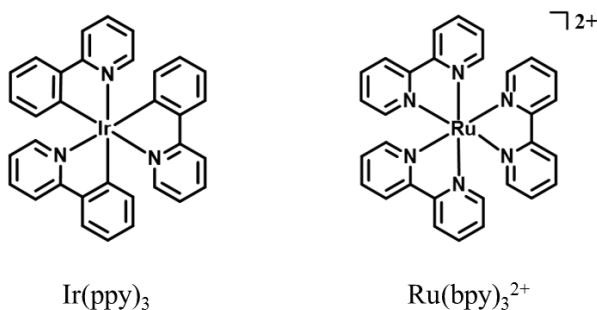

$Ir(ppy)_3$ $Ru(bpy)_3^{2+}$

Figure 3 ECL-active luminophores (inorganic systems)

that of Ru(bpy)$_3^{2+}$.[20] A blue-emitting Ir(III) complex, [Ir(df-ppy)$_2$(ptb)]$^+$, was also reported by Francis et al. It exhibited a strong blue-ECL signal with control of the HOMO/LUMO energy levels.[21]

In 2005, Kim, H. and Lee, J.-K. et al. reported diverse Ir(III) complex ECL systems which produce high ECL signals with TPA as a coreactant.[20] Among them, (pq)$_2$Ir(acac) and (pq)$_2$Ir(tmd) with TPA showed very high ECL emissions compared to a Ru(bpy)$_3^{2+}$/TPA system.
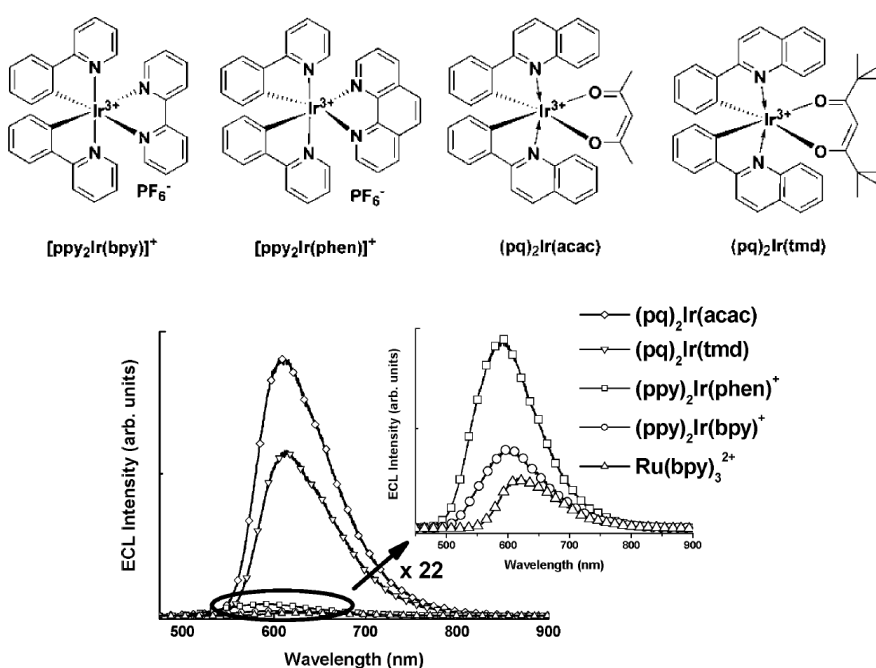
Figure 4 The structures and ECL spectra of Ir(III) complexes
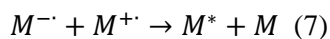
They suggest three ideal conditions for efficient ECL using diverse Ir(III) complexes. In the equations below, the electron-transfer reactions (3, 5, and 7) should be effective enough to generate high ECL emissions. Given that the direct oxidation of TPA on an electrode (reaction 2) occurs relatively slowly, whereas an emitter (reaction 1) can be oxidized relatively rapidly, the oxidation potential of the emitter should be sufficiently positive for the effective generation of TPA$^{\cdot}$.

$$\mathrm{M} - e^- \rightarrow M^{+\cdot} \quad (1)$$

$$\mathrm{TPA} - e^- \rightarrow TPA^{+\cdot} \quad (2)$$

$$M^{+\cdot} + TPA \rightarrow M + TPA^{+\cdot} \quad (3)$$

$$TPA^{+\cdot} \rightarrow TPA^{\cdot} + H^+ \quad (4)$$

$$M^{+\cdot} + TPA^{\cdot} \rightarrow M^* + side\ product \quad (5)$$

$$M + TPA^{\cdot} \rightarrow M^{-\cdot} + side\ product \quad (6)$$

$$M^{-\cdot} + M^{+\cdot} \rightarrow M^* + M \quad (7)$$

$$M^{-\cdot} + TPA^{+\cdot} \rightarrow M^* + \mathrm{TPA} \quad (8)$$

$$M^* \rightarrow M + h\upsilon \quad (9)$$
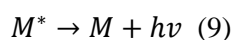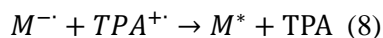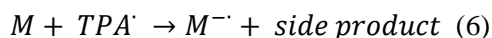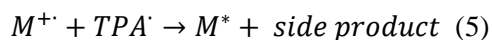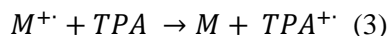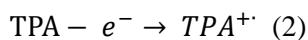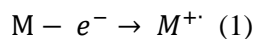
Reactions which form excited states (reaction 5 and 7) are also important steps to emit intense ECL. The reducing power of TPA$^{\cdot}$ was reported by the Bard group in ECL quenching experiments $(\epsilon^o(TPA^{\cdot}) = \sim -1.7\ V)$. The LUMO of the cation radical of the emitter should be lower than the potential of TPA$^{\cdot}$ for the efficient generation of M*. ECL can also be generated by an additional emitting pathway in a process known as annihilation. If the potential of TPA$^{\cdot}$ is more negative than the reduction potential of an anion radical emitter, equation 6 becomes effective, thus allowing the emission via annihilation.
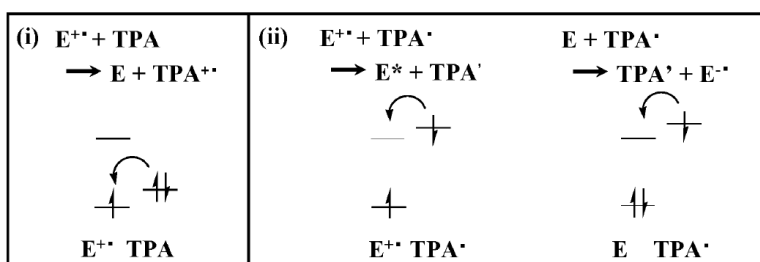

Figure 5 Postulated efficient ECL route

A.3 ECL Chemosensors Based on Cyclometalated Ir(III) Complexes

Although various Ir(III) complexes have been reported as ECL luminophores, only a few ECL chemosensors based on cyclometalated Ir(III) complexes have been developed. Most of existing ECL probes are based on ruthenium complex derivatives due to their well-studied optical and electrical properties, good solubility, and high ECL efficiency.

The Schmittel group has published several studies of ECL probes based on a cyclometalated Ir(III) complex. In 2010, they reported an iridium complex as a dual-channel lab-on-a-molecule for anion sensing.[22] Iridium dimer **A-1** did not show any PL and ECL emission; however, it showed a PL signal in the presence of cyanide and an ECL signal in the presence of acetate, respectively.

A-1
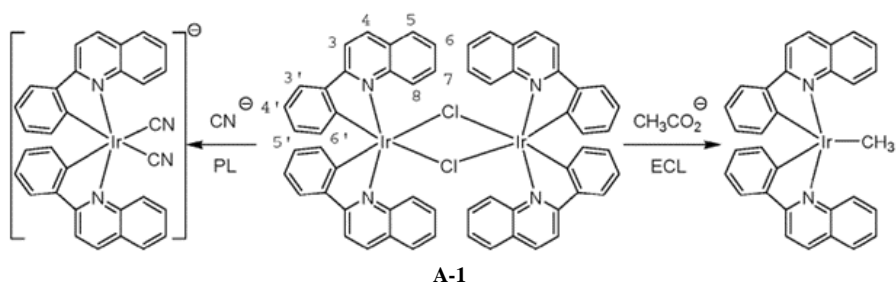
Figure 6 Iridium chloro-bridge dimer for anion sensing by PL and ECL dual channel.

A similar type of triple-channel probe was also reported by the Schmittel group in 2013.[23] They developed an Ir(III) complex **A-2** as a triple-channel lab-on-a-molecule for amino acid detection. Cysteine and homocysteine reacted with an aldehyde group on the ancillary ligand, leading to thiazolidine and thiazinane units provided. The formation of ring structures

induced a UV-vis absorbance change and PL enhancement. In the ECL channel, the electron-rich amino acid tryptophan can be oxidized more easily than **A-2** and can thus quench the ECL emission of **A-2** by disturbing the formation of excited states.
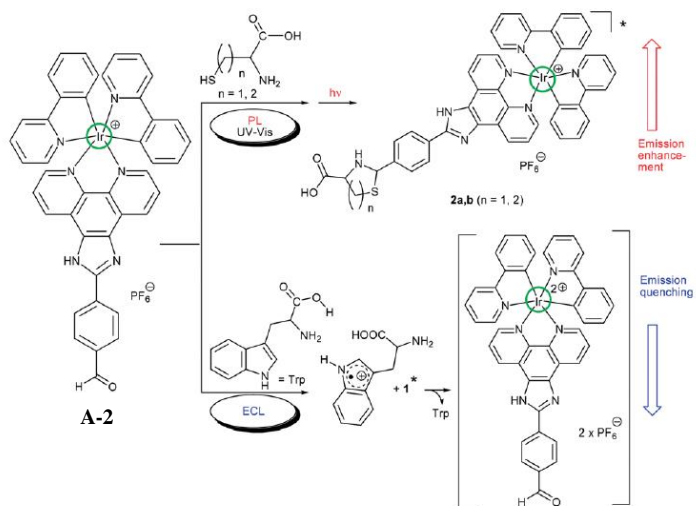

Figure 7 Ir(III) complex 1 as a lab-on-a-molecule for cysteine, homocysteine, and tryptophan.

A. 4 References

1. Richer, M. M. *Chem. Rev.,* **2004**, *104*, 3003-3036.

2. W. Miao, *Chem. Rev.,* **2008**, *108*, 2506-2553.

3. Qi, H.; Peng, Y.; Gao, Q.; Zhang, C. Sensors, **2009**, *9*, 674.

4. *Electrogenerated Chemiluminescence*; Bard, A. J. Ed.; Dekker: New York, 2004.

5. Hercules, D. M. *Science*, **1964**, *143*, 308.

6. Santhanam, K. S. V.; Bard, A. J. *J. Am. Chem. Soc.* **1965**, *87*, 139.

7. Chang, M.-M.; Saji, T.; Bard, A. J. *J. Am. Chem. Soc.* **1977**, *99*, 5399.

8. Liu, X. Q.; Shi, L. H.; Shi, W. X.; Niu, H.; Li, J.; Xu, G. B. *Angew. Chem., Int. Ed.* **2007**, *46*, 421.

9. Nagasubramian, G.; Gioda, A. S.; Bard, A. J. *J. Electrochem. Soc.* **1981**, *128*, 2158.

10. Kerr, E.; Doeven, E. H.; Wilson, D. J. D.; Hogan, C. F.; Francis, P. S. *Analyst*, **2016**, *141*, 62.

11. Leland, J. K.; Powell, M. J. *J. Electrochem. Soc.* **1990**, *137*, 3127.

12. David J. Vinyard, Shujun Su and Mark M. Richter, *J. Phys. Chem. A*, **2008**, *112*, 8529–8533.

13. Lee, K.S.; Zu, Y.; Herrmann, A.; Geerts, Y.; Mullen, K.; Bard, A. J. *J. Am. Chem. Soc.* **1999**, *121*, 3513.

14. Nepomnyashchii, A. B.; Bard, A. J. *Acc. Chem. Res.* **2012**, *45*, 1844.

15. Tokel, N.; Bard, A. J. *J. Am. Chem. Soc.* **1972**, *94*, 2862.

16. Rubinstein, I.; Bard, A. J. *J. Am. Chem. Soc.* **1981**, *103*, 512.

17. White, H. S.; Bard, A. J. *J. Am. Chem. Soc.* **1981**, *104*, 6891.

18. Leland, J. K.; Powell, M. J. *J. Electroanal. Chem.* **1991**, *318*, 91.

19. Bruce, D.; Richter, M. M. *Anal. Chem.* **2002**, *74*, 1340-1342.

20. Kim, J. I.; Shin, I.-S.; Kim. H.; Lee, J.-K. *J. Am. Chem. Soc.* **2005**, *127*, 1614.

21. Barbanate, G.J.; Doeven, E. H.; Kerr, E.; Connell, T. U.; Donnelly, P. S.; White, J. M. Lopes, T. Laird, S. Wilson, D. J. D.; Barnard, P. J.; Hogan, C. F.; Francis, P. S. *Chem. Eur. J.* **2014**, *20*, 3322.

22. Lin, H.; Cinar, M. E.; Schmittel, M. *Dalton Trans.* **2010**, *39*, 5130-5138.

23. Chen, K.; Schmittel, M. *Analyst*, **2013**, *138*, 6742-6745.

B. Electrogenerated Chemiluminescence Probes for Sulfide Based on Cyclometalated Ir(III) Complexes

B.1 Introduction

Hydrogen sulfide (H_2S), a well-known toxic gas, has recently been recognized as an important gaseous signalling molecule.[1, 2] H_2S is generated endogenously from L-cysteine by several enzymes such as cystathionine γ-lyase (CSE),[3] cystathionine β-synthase (CBS),[4] and 3-mercaptopyruvate sulfur transferase (3-MST).[5] As a gasotransmitter, H_2S regulates various biological processes in cardiovascular,[6] central nervous,[7] immune,[8] and gastrointestinal[9] systems. In blood plasma, 10-100 μM of sulfide is considered the normal level.[10, 11] However, an abnormal level of H_2S is associated with some diseases, including Alzheimer's disease,[12] Down's syndrome, diabetes,[13] and liver cirrhosis.[14] Therefore, simple methods for selective detection of H_2S are required in order to diagnose various diseases that increase the plasma H_2S concentration to abnormal levels.

So far, various approaches have been studied for the detection of H_2S, such as electrochemical analysis,[15] gas chromatography,[16] and colorimetric[17] and fluorescent[18] assays. In particular, a large number of fluorescent chemodosimeters for H_2S were developed based on the strong reducing[19, 20] or nucleophilic[21, 22] properties of sulfide anions. However, fluorescent assays cannot be used for point-of-care (POC) detection due to the requirement of an additional optical source and bulky equipment.

Electrogenerated chemiluminescence (ECL) is a light-emitting process caused by the electron-transfer reaction between electrochemically generated radical species at the electrodes.[23] In comparison with conventional

fluorescent methods, the ECL method has many advantages, including no background optical signal, high sensitivity and no need of extra light sources, providing simple and miniaturized sensing tools.[23, 24] These features afford strong benefits in the development of POC detection sensors. ECL luminophores were developed using various phosphorescent heavy-metal complexes such as Ru(II),[25] Os(II),[26] Eu(III),[27] Re(I),[28] Pt(II),[29] and Ir(III).[30-32] Among them, Ir(III) complexes have attracted increasing attention because they exhibit high luminescence efficiency, good electrochemical stability, and easy tunability of the luminescent colour by modulating the substitution of ligands.[30-32]

B.2 Results and Discussion

Design of Probes

We designed two ECL chemodosimetric probes for the sulfide anion based on Ir(III) complexes (Scheme 1). We selected (piq)2Ir(pic) (piq = 1-phenylisoquinoline, pic = picolinate) as a luminophore,[33] and the dinitrophenyl (DNP) group as a photo-induced electron transfer (PET) quencher[34] and a reaction site,[34-36] providing bright emission after the nucleophilic aromatic substitution (S_NAr) by the sulfide anion. Probe **1** has a DNP group on the ancillary ligand, while probe **2** has an additional quencher group on the main ligands that would further reduce the phosphorescent intensity of the probe itself and thus produce a high turn-on ratio in response to sulfide anions. Synthetic procedures of probes **1** and **2** are described in the supplementary material.
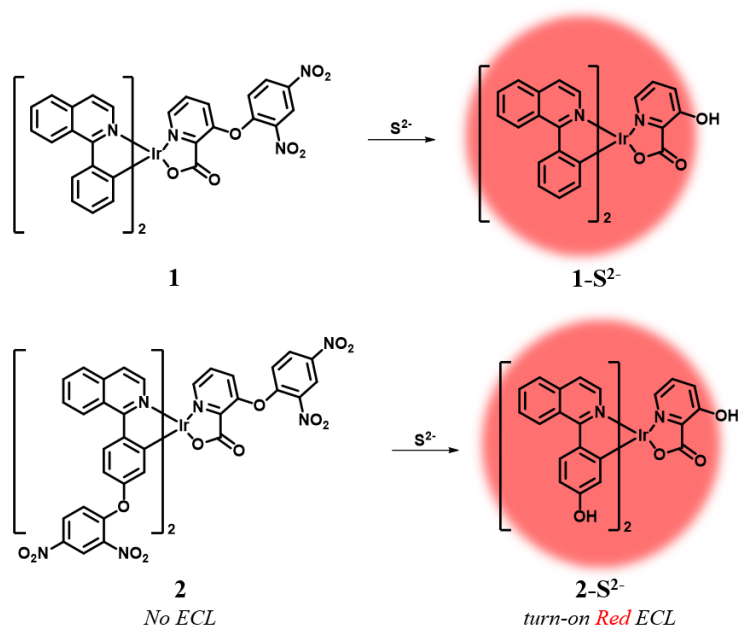
Scheme 1 Electrogenerated chemiluminescent sensing mechanism of probes **1** and **2**

Photoluminescence properties

We examined the phosphorescence spectra of probes **1** and **2**. As shown in Fig. 1a, the phosphorescence intensity of **1** gradually increased at 606 nm (λ_{ex} = 460 nm) until 10 equiv of sulfide anion (100 μM) was added. The phosphorescence intensity of **2** increased more dramatically than **1** at 601 nm (Fig. 1b). Probe **2** required a larger amount of sulfide anion (150 μM, 15 equiv.) than **1** for saturation because the former has more reaction sites for sulfide. The
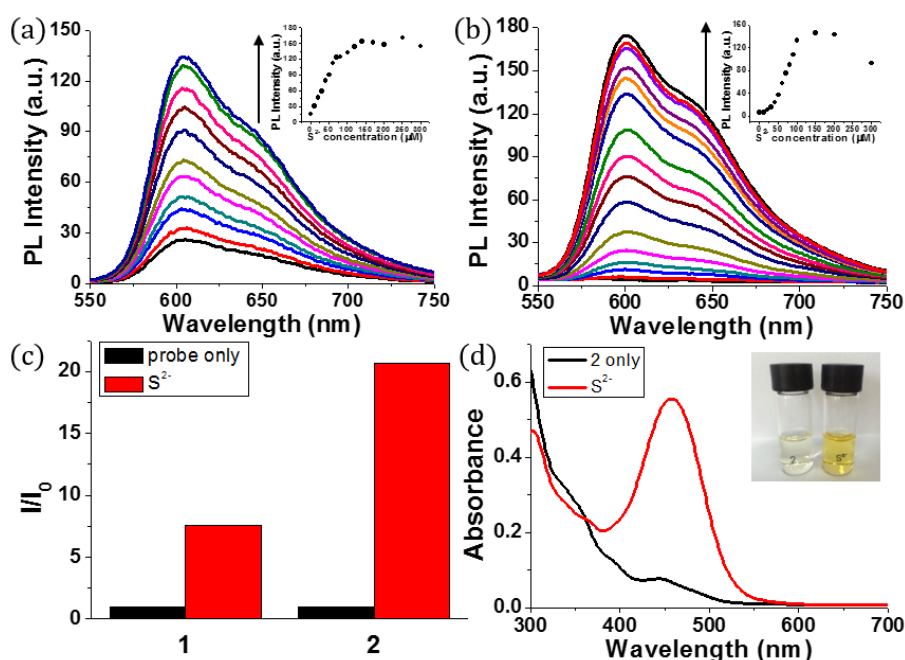

Figure 8 (a) Phosphorescent emission spectra of **1** (10 μM) in the presence of 0-100 μM of sulfide in CH₃CN (inset: Changes in phosphorescence intensity of **1** at 606 nm upon the addition of sulfide) (b) Phosphorescent emission spectra of **2** (10 μM) in the presence of 0-150 μM of sulfide in CH₃CN (inset: Changes in phosphorescent intensity of **2** upon the addition of sulfide) (c) Turn-on ratio of **1** and **2** in the absence (black bar) and presence (red bar) of 100 μM sulfide in CH₃CN (d) UV-vis absorption of **2** (10 μM) before and after addition of sulfide (100 μM) in CH₃CN.

14

estimated limit of detection (LOD) was calculated to be 1.9 μM for **1** and 0.2 μM for **2** (signal-to-noise (S/N) ratio = 3). Then, we compared the phosphorescence turn-on ratios of **1** and **2** in the presence of 100 μM of sulfide anion (Fig. 1c). The turn-on ratio of **2** was greater than **1**, as we expected. UV-vis absorption spectra were also investigated (Fig. 1d). In the presence of sulfide (10 equiv.), the absorption peak around 457 nm increased significantly. Probe **2** solution showed the corresponding color change from colorless to yellow, enabling colorimetric detection through the naked eye.

Theoretical calculations

Density functional theory (DFT) calculations supported the PET sensing mechanism of the probes (Fig. 2). The HOMOs of **1** and **2** were mainly localized on the Ir(III) center and phenyl ring of piq and the LUMO is localized
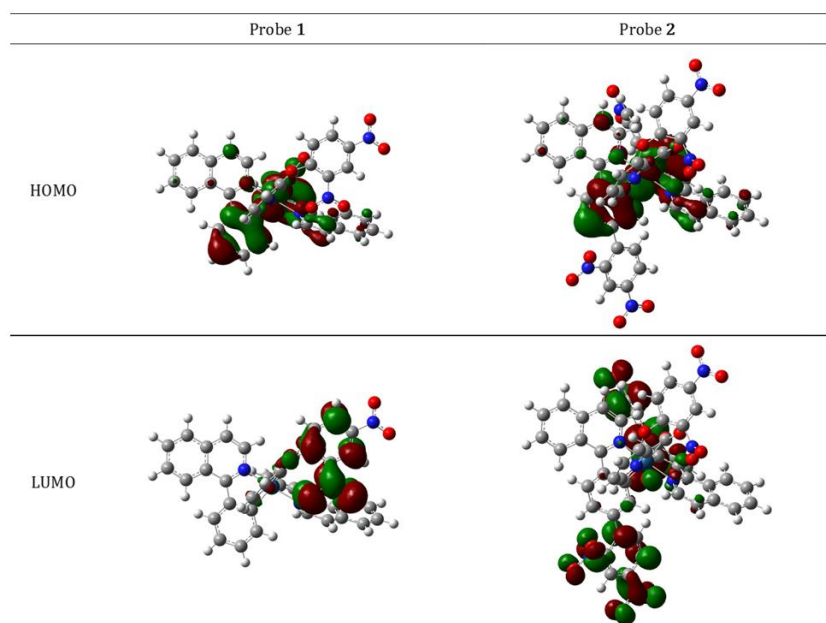

Figure 9 Electronic distributions of probes **1** and **2** from DFT calculations.

on the DNP, whereas the LUMO of Ir(III) complexes is generally localized on the isoquinoline of the main ligands. Hence, we expected that probes **1** and **2** were able to show an "off-on" emission signal in response to sulfide through the PET modulation. We also conducted cyclic voltammetry (CV) measurements and compared the HOMO/LUMO energy levels of luminophores (**1**-S^{2-} and **2**-S^{2-}) with the LUMO of a quencher (1-chloro-2,4-dinitrobenzene) to confirm the PET mechanism experimentally (Fig. 3). As expected, the LUMO (-4.36 eV) of the quencher is located between the HOMO (-5.35 eV) and LUMO (-3.08 eV) of **1**-S^{2-} as well as the HOMO (-5.19 eV) and LUMO (-2.87 eV) of **2**-S^{2-}. Therefore, the phosphorescence signal of the probes was quenched by the PET process before the cleavage of the DNP moiety from Ir(III) complexes upon the addition of sulfide.
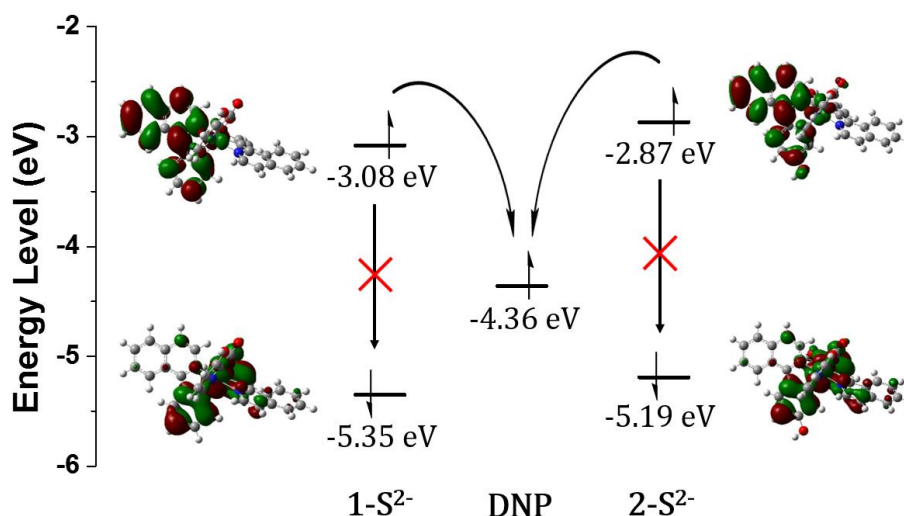

Figure 10 HOMO/LUMO energy levels calculated from CV measurements and electronic distributions of **1**-S^{2-} and **2**-S^{2-} and photo-induced electron transfer pathway.

16

PL selectivity test

　　We performed PL selectivity tests by adding 100 μM of each anion to 10 μM of probe **1** and **2**, respectively. As expected, only sulfide induced significant phosphorescence intensity of **1** at 606 nm (Fig. 4). Various anions, including F^-, Cl^-, Br^-, I^-, HCO_3^-, CO_3^{2-}, $C_2O_4^{2-}$, SO_4^{2-}, NO_3^-, N_3^-, AcO^-, SCN^- and CN^- and biothiols such as cysteine (Cys), homocysteine (Hcy) and glutathione (GSH) could not show phosphorescence change under the same condition with **1** (Fig. 4). Probe **2** also exhibited a dramatic increase upon the addition of sulfide, whereas other analytes could not induce any remarkable responses (Fig. 5).

Figure 4 PL responses of **1** (10 μM) in the presence of various analytes (100 μM) in CH_3CN. (25 mM TPA, and 0.1 M $TBAPF_6$ as the supporting electrolyte) (a) probe only, (b) F^-, (c) Cl^-, (d) Br^-, (e) I^-, (f) HCO_3^-, (g) CO_3^{2-}, (h) $C_2O_4^{2-}$, (i) SO_4^{2-}, (j) NO_3^-, (k) N_3^-, (l) AcO^-, (m) SCN^-, (n) CN^-, (o) Cys, (p) Hcy, (q) GSH, (r) S^{2-}.
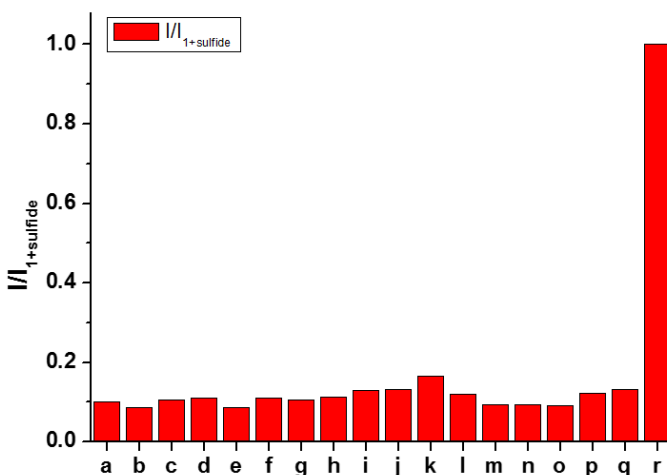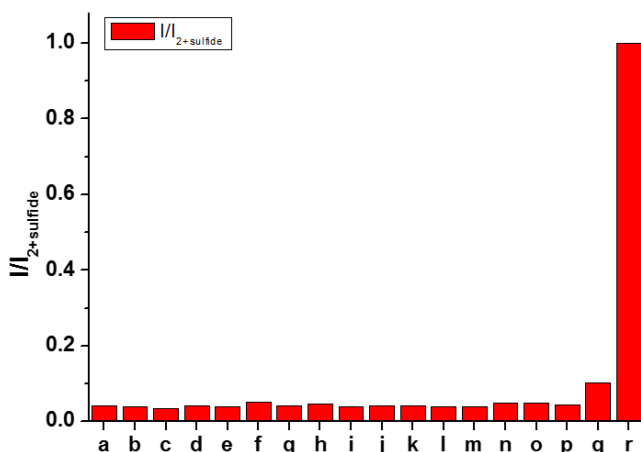
Figure 5 PL responses of **2** (10 μM) in the presence of various analytes (100 μM) in CH$_3$CN. (25 mM TPA, and 0.1 M TBAPF$_6$ as the supporting electrolyte) (a) probe only, (b) F$^-$, (c) Cl$^-$, (d) Br$^-$, (e) I$^-$, (f) HCO$_3^-$, (g) CO$_3^{2-}$, (h) C$_2$O$_4^{2-}$, (i) SO$_4^{2-}$, (j) NO$_3^-$, (k) N$_3^-$, (l) AcO$^-$, (m) SCN$^-$, (n) CN$^-$, (o) Cys, (p) Hcy, (q) GSH, (r) S^{2-}.

Electrogenerated Chemiluminescence properties

The ECL measurements were performed during the CV process. Probe **1** itself showed the initial ECL intensity at around 1.4 V, but further increase in the ECL intensity of **1** was observed in the presence of sulfide (Fig. 6a). A titration curve of **1** was obtained against various concentrations of the sulfide anion (Fig. 6b). A linear relationship between the ECL intensity and the sulfide concentration was observed from 0 to 80 μM of sulfide. The estimated LOD was calculated to be 27 nM, significantly lower than the LOD of phosphorescence. Hence, **1** can be used as a highly sensitive ECL sensor to detect abnormal levels of H$_2$S.

A similar turn-on ECL of **2** was observed in the presence of sulfide (Fig. 6c). Probe **2** showed 3-fold enhancement of the ECL intensity at around

1.6 V in the presence of 15 equiv. of sulfide (150 μM). The emission signal increased greatly when the sulfide concentration was in the range of 0–100 μM (Fig. 6d). Although the ECL turn-on ratio of **2** was greater than that of **1**, the absolute ECL intensity of **2** was low even after saturation with sulfide (Fig. 7). The maximum signal of **2** was only 5.7% of **1** in the presence of sulfide (80 μM, 8 equiv.). The low ECL intensity of **2** caused low sensitivity toward the sulfide
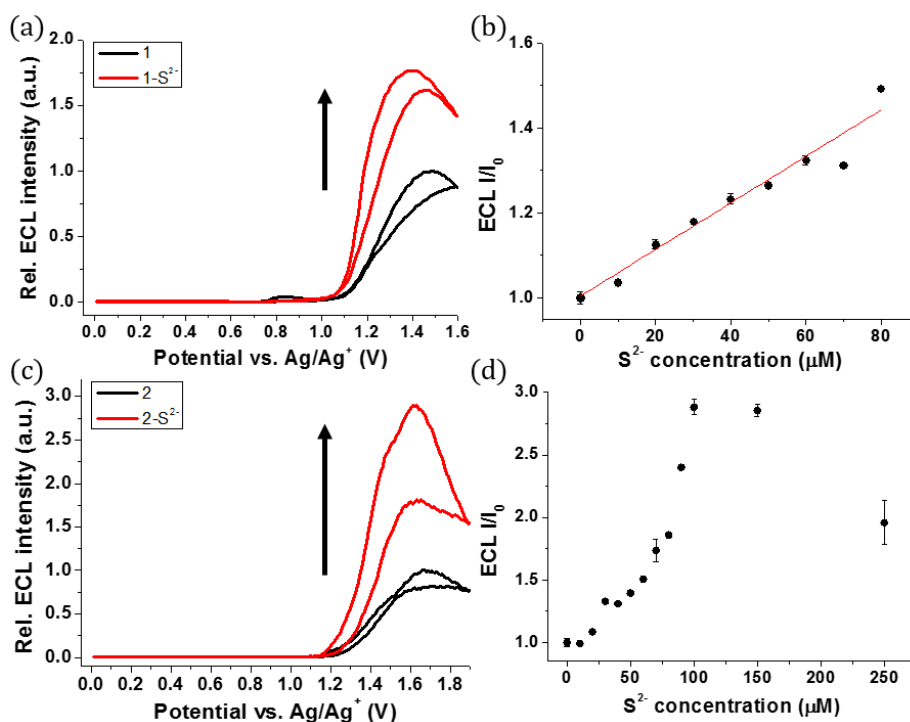

Figure 6 (a) ECL intensity of **1** (10 μM) upon the addition of sulfide (80 μM) in CH_3CN (25 mM TPA, and 0.1 M $TBAPF_6$ as the supporting electrolyte) (b) ECL titration curve of **1** (10 μM) upon the addition of sulfide in CH_3CN (10 mM TPA, and 0.1 M $TBAPF_6$ as the supporting electrolyte) (c) ECL intensity of **2** (10 μM) upon the addition of sulfide (150 μM) in CH_3CN (25 mM TPA, and 0.1 M $TBAPF_6$ as the supporting electrolyte) (d) ECL titration curve of **2** (10 μM) upon the addition of sulfide in CH_3CN (10 mM TPA, 0.1 M $TBAPF_6$ as the supporting electrolyte) (The potential is swept at a Pt disk electrode (diameter: 2 mm) vs Ag/Ag$^+$, scan rate: 0.1 V/s)
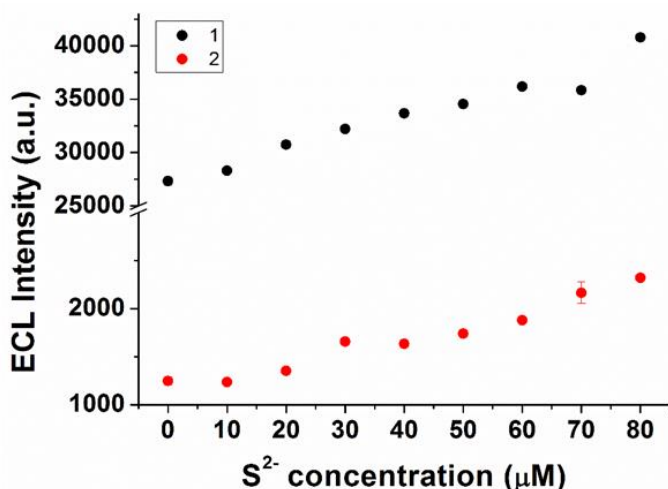
Figure 7 ECL intensity of 10 μM **1** and **2** upon the addition of sulfide in CH₃CN (10 mM TPA, 0.1 M TBAPF₆ as the supporting electrolyte, and the potential is swept at a Pt disk electrode (diameter: 2 mm) vs Ag/Ag⁺, scan rate: 0.1 V/s)

anion, and the estimated LOD of **2** was calculated to be 0.3 μM, which is relatively high compared to that of **1**.

Electrochemical studies for ECL mechanism

The low ECL intensity of **2** can be explained by the CV measurements (Fig. 8). We compared the HOMO/LUMO energy levels of **1**-S^{2-} and **2**-S^{2-} calculated from CV measurements with the HOMO of tri-*n*-propylamine (TPA). One of the conditions for the efficient ECL emission is that the HOMO of the emitter should be lower than that of TPA for an efficient generation of TPA$^{+\cdot}$.[37] The HOMO energy level of **1**-S^{2-} (-5.35 eV) is relatively well matched with that of TPA (-5.38 eV), so that 1 can emit a strong ECL in response to the sulfide anion through the relatively smooth electron transfer from TPA HOMO to **1**-S^{2-} HOMO. In contrast, the HOMO energy level of **2**-S^{2-} (-5.19 eV) is quite higher than that of TPA because the hydroxyl groups on the main ligands destabilized
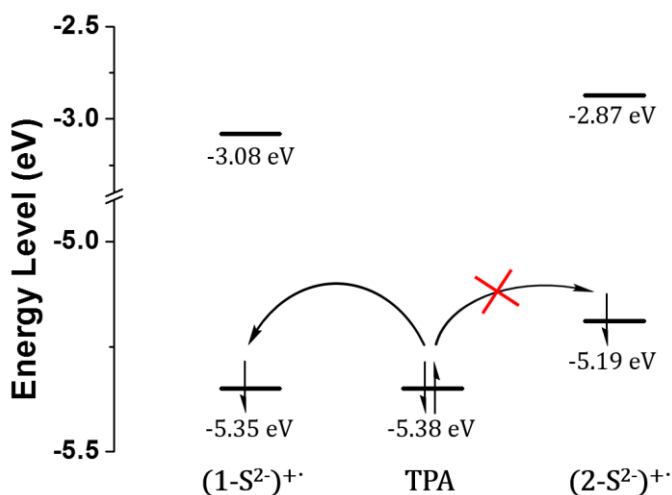
Figure 8 HOMO/LUMO energy levels calculated from CV measurements and generation of TPA[+.] through the catalytic pathway.

the HOMO level. Thus, the electron transfer from TPA to 2-S^{2-} hardly occurred, causing a weak ECL emission. The CV studies rationalized the low ECL intensity of **2**. Furthermore, the energy level of the TPA radical is higher than that of the LUMO of (1-S^{2-})$^{+.}$ or (2-S^{2-})$^{+.}$, so that the excited state of (1-S^{2-})$^{+.}$ or (2-S^{2-})$^{+.}$ can be easily formed to generate the ECL.[38]

ECL selectivity test

The selectivity of **2** was tested by adding 100 μM of each anion to 10 μM of probe **2** (Fig. 9). Only the sulfide anion induced a significant increase in the ECL intensity, whereas almost no ECL changes were observed upon the addition of other anions. In particular, CN^{-} and biothiols such as Cys, Hcy, and GSH, which are difficult to be distinguished from sulfide, could not increase the emission intensity. These results suggest that probe **2** is a highly selective probe for H$_2$S over other analytes and can be used for biological applications based on ECL analysis.
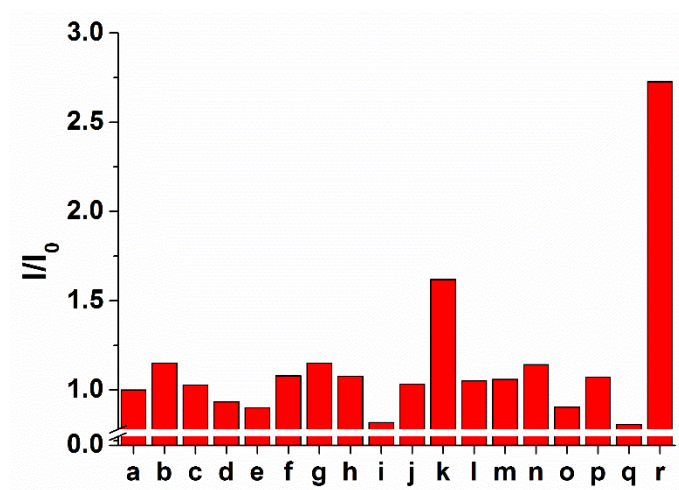
Figure 11 ECL responses of **2** (10 μM) in the presence of various analytes (100 μM) in CH₃CN. (25 μM TPA, and 0.1 M TBAPF₆ as the supporting electrolyte) (a) probe only, (b) F⁻, (c) Cl⁻, (d) Br⁻, (e) I⁻, (f) HCO₃⁻, (g) CO₃²⁻, (h) C₂O₄²⁻, (i) SO₄²⁻, (j) NO₃⁻, (k) N₃⁻, (l) AcO⁻, (m) SCN⁻, (n) CN⁻, (o) Cys, (p) Hcy, (q) GSH, (r) S²⁻.

B.3 Conclusion

We designed two "off-on" chemodosimetric ECL probes for H₂S, based on cyclometalated Ir(III) complexes. In the presence of sulfide anions, the ECL intensity of probe **2** increased greatly due to the blocking of the PET quenching process. Furthermore, the probe showed a high turn-on ratio with H₂S only. We expect that our rational sensing approach will pave the way for the development of various ECL-based sensing tools for small biomolecules.

B.4 Experimental Section

B.4.1 Instrumentation and materials

All the chemicals were purchased from Sigma-Aldrich (Sigma-Aldrich Corp., MO, USA), TCI (Tokyo Chemical Industry, Tokyo, Japan) or Alfa (Alfa Aesar, MA, USA) and used without any further purification. Thin layer chromatography was performed using Merck silica gel 60F-254 on aluminum foil. SiliaFlash® P60 (230-400 mesh) from SILICYCLE was used for stationary phase in chromatographic separation. All the ^{1}H and ^{13}C NMR spectra were obtained from Bruker Advance DPX-300. Chemical shifts (δ) were reported as ppm (in CDCl$_3$ or DMSO). GC-MS (Gas Chromatography-Mass Spectrometer) was performed on JMS 6890 Series, with EI-positive mode. Absorption spectra were measured on a DU 800 Series. Fluorescence emission spectra were obtained on a JASCO FP-6500 spectrometer and the slit width was 5 nm for excitation and emission. The probe **1** and **2** solution for all the photophysical experiment were prepared from 2 mM stock solution in DMSO, diluted with acetonitrile and stored in a refrigerator for use. The Na$_2$S generating sulfide anion was dissolved in CH$_3$CN containing 10 % of HEPES. (DMSO = dimethyl sulfoxide)

B.4.2 Synthesis of compounds
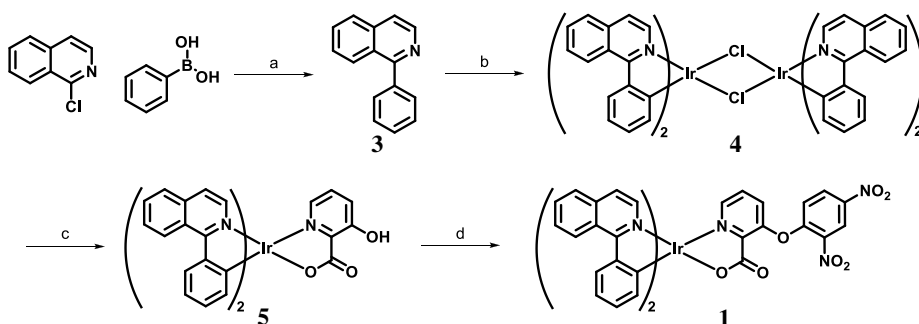
Scheme 2 a) K_2CO_3, $Pd(PPh_3)_4$, H_2O, THF, reflux; b) $IrCl_3 \cdot xH_2O$, 2-ethoxyethanol, H_2O, reflux; c) 3-hydroxypicolinic acid, Na_2CO_3, 2-ethoxyethanol, 50 °C; d) 1-chloro-2,4-dinitrobenzene, K_2CO_3, DMF, reflux. (THF = tetrahydrofuran, DMF = dimethyl formamide)

Synthesis of 3

1-Chloroisoquinoline (1000 mg, 6.1 mmol), phenylboronic acid (970 mg, 7.9 mmol), K_2CO_3 (2500 mg, 18 mmol) and $Pd(PPh_3)_4$ (140 mg, 0.12 mmol) were dissolved in a mixture of THF (30 mL) and H_2O (30 mL). After stirring overnight at 80°C, the reaction mixture was cooled down to room temperature and extracted with CH_2Cl_2 and water. The organic layer was dried over anhydrous Na_2SO_4, filtered, concentrated, and the residue was purified by silica gel column chromatography with hexane/ethyl acetate (5:1 v/v) as the eluent to give compound **3** (940 mg, 4.6 mmol, 75 %): ^{1}H NMR (300 MHz, CDCl₃) δ 7.50-7.59 (4H, m), 7.65-7.75 (4H, m), 7.90 (1H, d, J=8.2Hz), 8.13 (1H, d, J=8.5Hz), 8.64 (1H, d, J=5.7Hz).

Synthesis of 5

Iridium(III) chloride hydrate $IrCl_3 \cdot xH_2O$ (170 mg, 0.6 mmol) and compound **3** (300 mg, 1.5 mmol) were dissolved in a mixture of 2-ethoxyethanol (15 mL) and H_2O (5 mL). The mixture as the heated at reflux for 24h. The solution was cooled to room temperature, and water (100 mL) added. The red precipitate was filtered, washed with water, and the dried under IR lamp. The dimeric precursor was isolated as a red powder (210 mg, 0.16 mmol, 55 %). Dimer **4** (41 mg, 0.03 mmol), 3-hydroxypicolinic acid (21 mg, 0.15 mmol) and Na_2CO_3 (16 mg, 0.15 mmol) were dissolved in 2-ethoxyethanol (3 mL) and heated at 50°C for 45 min. After cooling down, the solvent was evaporated under reduced pressure. The residue was re-dissolved in CH_2Cl_2 and washed with water. The crude compound was purified by silica gel column chromatography with CH_2Cl_2/methyl alcohol (50:1 v/v) as the eluent to afford compound **5** (41 mg, 0.055 mmol, 92 %): ^1H NMR (300 MHz, $CDCl_3$) δ 6.24 (1H, d, J=7.5Hz), 6.50 (1H, d, J=7.6Hz), 6.73 (1H, t, J=7.3Hz), 6.80 (1H, t, J=7.4Hz), 6.96 (1H, t, J=7.3Hz), 7.03 (1H, t, J=7.4Hz), 7.46 (1H, d, J=6.4Hz), 7.53 (1H, d, J=6.4Hz), 7.73-7.77 (4H, m), 7.88-7.97 (2H, m), 8.21 (1H, d, J=8.0Hz), 8.27 (1H, d, J=8.0Hz), 8.66 (1H, d, J=6.4Hz), 8.96-8.99 (2H, m), 13.8 (1H, s)

Synthesis of 1

Compound **5** (57 mg, 0.076 mmol), 1-chloro-2,4-dinitrobenzene (46 mg, 0.23 mmol) and K_2CO_3 (32 mg, 0.23 mmol) were dissolved in 3 mL of DMF, and the mixture was heated to reflux for 1 h 30 min. The reaction mixture was cooled at room temperature, concentrated in vacuo to remove all volatiles, diluted with CH_2Cl_2, added H_2O, and extracted with CH_2Cl_2 twice. The combined organic extracts were dried over Na_2SO_4, filtered, and evaporated.

The crude compound was purified by silica gel column chromatography with CHCl$_3$/acetone (15:1 v/v) as the eluent to give a desired product (53 mg, 0.06 mmol, 77 %): ^{1}H NMR (300 MHz, CDCl3) δ 6.14 (1H, d, J=7.6Hz), 6.56 (1H, d, J=7.5Hz), 6.70 (1H, t, 7.3Hz), 6.76 (1H, d, J=9.2Hz), 6.83 (1H, t, J=7.2Hz), 6.94 (1H, t, J=7.3Hz), 7.06 (1H, t, J=7.2Hz), 7.36 (1H, d, J=6.4Hz), 7.42-7.46 (2H, m), 7.55 (1H, d, J=6.4Hz), 7.68-7.80 (6H, m), 7.91-8.01 (2H, m), 8.18 (1H, d, J=8.0Hz), 8.24 (1H, dd, J=9.2Hz, 2.7Hz), 8.30 (1H, d, J=8.0Hz), 8.68 (1H, d, J=6.4Hz), 8.90 (1H, d, J=2.6Hz), 8.93-9.02 (2H, m). GC-MS (FAB[+]) [M=C$_{42}$H$_{26}$IrN$_5$O$_7$], calculated 905.1462, found 905.1464.
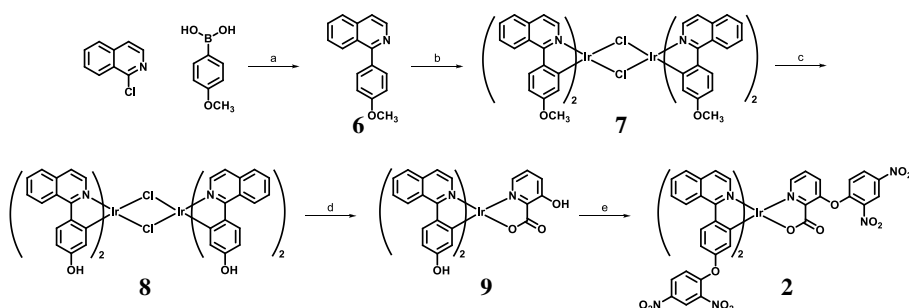
Scheme 3 a) Pd(PPh$_3$)$_4$, Na$_2$CO$_3$, toluene, H$_2$O, ethyl alcohol, reflux; b) IrCl$_3$·xH$_2$O, 2-ethoxyethanol, H$_2$O, reflux; c) BBr$_3$, DCM, 0 °C → r.t; d) 3-hydroxypicolinic acid, Na$_2$CO$_3$, 2-ethoxyethanol, 50 °C; e) 1-chloro-2,4-dinitrobenzene, K$_2$CO$_3$, DMF, reflux. (DCM = dichloromethane)

Synthesis of 6

A two-neck round bottom flask was charged with a 1-chloroisoquinoline (200 mg, 1.2 mmol), 4-methoxyphenylboronic acid (240 mg, 1.6 mmol), Na$_2$CO$_3$ (910 mg, 8.5 mmol) and Pd(PPh$_3$)$_4$ (42 mg, 0.04 mmol), and toluene (5 mL),

H$_2$O (5 mL), and ethyl alcohol (1 mL) were sequentially added. The reaction mixture was refluxed for 8 h, and then cooled to room temperature. To the reaction mixture was added aqueous NH$_4$Cl (10 mL), extracted by ethyl acetate for three times, dried over anhydrous Na$_2$SO$_4$, filtered, and evaporated in vacuum to afford the crude product. The crude was purified by silica gel column chromatography with hexane/ethyl acetate (5:1 v/v) as the eluent to give compound **6** (230 mg, 1 mmol, 82 %): ^{1}H NMR (300 MHz, CDCl$_3$) δ 3.93 (1H, s), 7.10 (1H, d, J=8.6Hz), 7.56 (1H, t, J=7.1Hz), 7.64 (1H, d, J=5.7Hz), 7.68-7.74 (3H, m), 7.90 (1H, d, J= 8.2Hz), 8.17 (1H, d, J=8.5Hz), 8.61 (1H, d, J=5.7Hz).

Synthesis of 9

Iridium(III) chloride hydrate IrCl$_3$·xH$_2$O (430 mg, 1.4 mmol) and compound **6** (840 mg, 3.6 mmol) were dissolved in a mixture of 2-ethoxyethanol (21 mL) and H$_2$O (7 mL). The mixture as the heated at reflux for 24h. The solution was cooled to room temperature, and water (100 mL) added. The precipitate was filtered, washed with water, and the dried under IR lamp. The crude product was used for the next step without further purification. To a stirred solution of **7** (630 mg, 0.45 mmol) in CH$_2$Cl$_2$ (7 mL) at 0 °C, BBr$_3$ (2.7 mL, 1.0 M solution in CH$_2$Cl$_2$) was added dropwise via syringe. The reaction was allowed to stir at room temperature overnight. The reaction was quenched slowly with MeOH (10 mL), diluted with CH$_2$Cl$_2$, and neutralized with saturated NaHCO$_3$ solution. The volatiles were removed under vacuum, and then the residue was re-dissolved in CH$_2$Cl$_2$ and poured H$_2$O (100 mL) with stirring. The precipitate was collected by filtration and used without further purification. The formation of compound **8** was determined by ^{1}H NMR in

DMSO, which showed disappearance of a singlet peak of methoxy hydrogen (δ 3.93, 3H, s). Compound **8** (610 mg, 0.5 mmol), 3-hydroxypicolinic acid (200.5 mg, 1.4 mmol) and Na_2CO_3 (152.6 mg, 1.4 mmol) were dissolved in 2-ethoxyethanol (15 mL) and heated at 50°C for 1 h 30 min. After cooling down, the solvent was evaporated under reduced pressure. The residue was re-dissolved in CH_2Cl_2 and washed with water. The crude compound was purified by silica gel column chromatography with CH_2Cl_2/methyl alcohol (50:1 v/v) as the eluent to afford compound **9** (180 mg, 0.23 mmol, 16 %): ^{1}H NMR (300 MHz, $CDCl_3$) δ 5.67 (1H, d, J=2.5Hz), 5.92 (1H, d, J=2.6Hz), 6.50 (1H, dd, J=8.7Hz, 2.6Hz), 6.58 (1H, dd, J=8.7Hz, 2.6Hz), 7.16-7.20 (2H, m), 7.24 (1H, d, J=6.5Hz), 7.33-7.40 (2H, m), 7.44 (1H, d, J=6.4), 7.71-7.75 (4H, m), 7.85-7.88 (1H, m), 7.90-7.93 (1H, m), 8.14 (1H, d, J=8.8Hz), 8.20 (1H, d, J=8.8Hz), 8.56 (1H, d, J=6.4Hz), 8.88-8.90 (2H, m), 13.78 (1H, s)

Synthesis of 2

Compound **9** (180 mg, 0.23 mmol), 1-chloro-2,4-dinitrobenzene (140 mg, 0.7 mmol) and K_2CO_3 (95 mg, 0.7 mmol) were dissolved in 10 mL of DMF, and the mixture was heated to reflux for 1 h 30 min. The reaction mixture was cooled at room temperature, concentrated in vacuo to remove all volatiles, diluted with CH_2Cl_2, added H_2O, and extracted with CH_2Cl_2 twice. The combined organic extracts were dried over Na_2SO_4, filtered, and evaporated. The crude compound was purified by silica gel column chromatography with hexane/ethyl acetate (2:1 v/v) to only ethyl acetate as the eluent to give compound **2** (56 mg, 0.04 mmol, 19 %): ^{1}H NMR (300 MHz, $CDCl_3$) δ 6.76 (1H, dd, J=8.7Hz, 2.5Hz), 6.80 (1H, d, J=9.2Hz), 6.88 (1H, dd, J=8.7Hz, 2.5Hz), 6.95 (1H, d, J=9.2Hz), 7.04 (1H, d, J=9.2Hz), 7.34 (2H, s), 7.44 (1H, d,

J=6.4Hz), 7.53-7.58 (1H, m), 7.69-7.86 (9H, m), 8.04 (1H, dd, J=9.2Hz, 2.7Hz), 8.13 (1H, dd, J=9.2Hz, 2.7Hz), 8.18 (1H, d, J=8.8Hz), 8.25 (1H, dd, J=9.1Hz, 2.7Hz), 8.34 (1H, d, J=8.8Hz), 8.50 (1H, d, J=2.7Hz), 8.53 (1H, d, J=6.4Hz), 8.63 (1H, d, J=2.7Hz), 8.72-8.75 (1H, m), 8.85 (1H, d, J=2.5Hz). GC-MS (FAB$^+$) [M = $C_{54}H_{31}IrN_9O_{17}$], calculated 1270.1467, found 1270.1472.

B.4.3 Electrochemical and electrogenerated chemiluminescent (ECL) measurements

Electrochemical study was performed with a CH Instruments 660 Electrochemical Analyzer (CH Instruments, Inc., TX, USA). In the electrochemical study, cyclic voltammetry (CV) was applied to individual solutions in order to investigate electrochemical oxidative and reductive behaviors. Particularly, a CH Instruments 650B Electrochemical Analyzer was used in ECL experiments to apply potential sweeps. The ECL intensity profile was obtained using a low-voltage photomultiplier tube module (H-6780, Hamamatsu photonics K.K., Tokyo, Japan) operated at 1.0 V. A 25 μL volume ECL cell was directly mounted PMT module with home-made mounting support during the experiments. All the ECL data were collected upon the simultaneous cyclic voltammetry on the solution. The ECL solutions commonly contained 10 mM TPA (tri-*n*-propylamine, Sigma-Aldrich, MO, USA) coreactant and 0.1 M tetrabutylammonium hexafluorophosphate (TBAPF$_6$, TCI) supporting electrolyte in acetonitrile (MeCN, spectroscopy grade, ACROS). Especially, TPA was selected and used as an ECL coreactant as it has been widely studied and known on its electrochemical properties. All the electrochemical and ECL experiments were referenced with respect to an Ag/Ag$_+$ reference electrode. All potential values were calibrated against the

saturated calomel electrode (SCE) by measuring the oxidation potential of 1 mM ferrocene (vs Ag/Ag$^+$) as a standard ($E^{o'}_{ox}$(Fc/Fc$^+$) = 0.424 V vs SCE). Cyclic voltammetry for ECL experiments was applied to the solutions at the scan rate of 0.1 V/s. The electrochemical and ECL solutions were freshly prepared in each experiment, and Pt working electrode was polished with 0.05 M alumina (Buehler, IL, USA) on a felt pad. Then the electrode was blown by ultra-pure N$_2$ gas for 1 min. A single solution was only used for one experimental try, and discarded after collecting data. The reported ECL values were obtained by averaging the values from at least three tries with a good reliability.

B.5 Reference

1. Gadalla, M. M. and Snyder, S. H. *J. Neurochem.*, **2010**, *113*, 14-26.

2. Kabil, O. and Banerjee, R. *J. Biol. Chem.,* **2010**, *285*, 21903-21907.

3. Sen, N.; Paul, B. D.; Gadalla, M. M.; Mustafa, A. K.; Sen, T.; Xu, R.; Kim S.; Snyder, S. H. *Mol. Cell*, **2012**, *45*, 13-24.

4. Singh, S.; Padovani, D.; Leslie, R. A.; Chiku, T.; Banerjee, R. *J. Biol. Chem.,* **2009**, *284*, 22457-22466.

5. Shibuya, N.; Yoshida, M.; Ogasawara, Y.; Togawa, T.; Ishii, K.; Kimura, H. *Antioxid. Redox Signaling,* **2009**, *11*, 703-714.

6. Calvert, J. W.; Jha, S.; Gundewar, S.; Elrod, J. W.; Ramachandran, A.; Pattillo, C. B.; Kevil C. G.; Lefer, D. J. *Circ. Res.*, **2009**, *105*, 365-374.

7. Abe K.; Kimura, H. *J. Neurosci.*, **1996**, *16*, 1066-1071.

8. Zanardo, R. C.; Brancaleone, V.; Distrutti, E.; Fiorucci, S.; Cirino G.; Wallace, J. L. *FASEB J.*, **2006**, *20*, 2118-2120.

9. Linden, D. R. *Antioxid. Redox Signaling*, **2014**, *20*, 818-830.

10. Papapetropoulos, A.; Pyriochou, A.; Altaany, Z.; Yang, G.; Marazioti, A.; Zhou, Z.; Jeschke, M. G.; Branski, L. K.; Herndon, D. N.; Wang, R.; Szabo, C. *Proc. Natl. Acad. Sci.,* **2009**, *106*, 21972.

11. Y. H. Chen, W. Z. Yao, B. Geng, Y. L. Ding, M. Lu, M. W. Zhao and C. S. Tang, *Chest*, **2005,** *128*, 3205-3211.

12. Eto, K.; Asada, T.; Arima, K.; Makifuchi, T.; Kimura, H. *Biochem. Biophys. Res. Commun.*, **2002**, *293*, 1485-1488.

13. Kamoun, P.; Belardinelli, M. C.; Chabli, A.; Lallouchi, K.; Chadefaux-Vekemans, B. *Am. J. Med. Genet. A*, **2003**, *116a*, 310-311.

14. Fiorucci, S.; Antonelli, E.; Mencarelli, A.; Orlandi, S.; Renga, B.; Rizzo, G.; Distrutti, E.; Shah V.; Morelli, A. *Hepatology*, **2005**, *42*, 539-548.

15. Lawrence, N. S.; Davis, J.; Jiang, L.; Jones, T. G. J.; Davies S. N.; Compton, R. G. *Electroanalysis*, **2000**, *12*, 1453-1460.

16. Radford-Knoery J.; Cutter, G. A. *Anal. Chem.,* **1993**, *65*, 976-982.

17. Bae, J.; Choi, M. G.; Choi. J; Chang, S.-K. *Dyes and Pigments*, **2013**, *99*, 748-752.

18. Yu, F.; Li, P.; Song, P.; Wang, B.; Zhao, J.; Han, K. *Chem. Commun.*, **2012**, *48*, 2852-2854.

19. Lippert, A. R.; New E. J.; Chang, C. J. *J. Am. Chem. Soc.*, **2011**, *133*, 10078-10080.

20. Peng, H.; Cheng, Y.; Dai, C.; King, A. L.; Predmore, B. L.; Lefer, D. J.; Wang, B. *Angew. Chem. Int. Ed.*, **2011**, *50*, 9672-9675.

21. Chen, Y.; Zhu, C.; Yang, Z.; Chen, J.; He, Y.; Jiao, Y.; He, W.; Qiu, L.; Cen, J.; Guo, Z. *Angew. Chem. Int. Ed.*, **2013**, *52*, 1688-1691.

22. Liu, C.; Pan, J.; Li, S.; Zhao, Y.; Wu, L. Y.; Berkman, C. E.; Whorton A. R.; Xian, M. *Angew. Chem. Int. Ed.*, **2011**, *50*, 10327-10329.

23. Richter, M. M. *Chem. Rev.*, **2004**, *104*, 3003-3036.

24. Miao, W. *Chem. Rev.*, **2008**, *108,* 2506-2553.

25. McCord P.; Bard, A. J. *J. Electroanal. Chem. Interfacial Electrochem.,* **1991**, *318*, 91-99.

26. Bruce, D.; Richter, M. M.; Brewer, K. J. *Anal. Chem.*, **2002**, *74*, 3157-3159.

27. Richter, M. M.; Bard, A. J. *Anal. Chem.*, **1996**, *68*, 2641-2650.

28. Richter, M. M.; Debad, J. D.; Striplin, D. R.; Crosby, G. A.; Bard, A. J. *Anal. Chem.*, **1996**, *68*, 4370-4376.

29. Gross, E. M.; Armstrong, N. R.; Wightman, R. M. *J. Electrochem. Soc.*, **2002**, *149*, E137.

30. You, Y.; Nam, W. *Chem. Soc. Rev.*, **2012**, *41*, 7061-7084.

31. Zhou, Y.; Gao, H.; Wang, X.; Qi, H.; *Inorg. Chem.*, **2015**, *54*, 1446-1453.

32. Li, M.-J.; Jiao, P.; Lin, M.; He, W.; Chen G.-N.; Chen, X. *Analyst*, **2011**, *136*, 205-210.

33. Fernandez-Hernandez, J. M.; Longhi, E.; Cysewski, R.; Polo, F.; Josel, H.-P.; De Cola, L. *Anal. Chem.*, **2016**, *88*, 4174-4178.

34. Cao, X.; Lin, W.; Zheng, K.; He, L. *Chem. Commun.*, **2012**, *48*, 10529-10531.

35. Liu, T.; Xu, Z.; Spring, D. R.; Cui, J. *Org. Lett.*, **2013**, *15*, 2310-2313.

36. Liu, Y.; Feng, G. *Org. Biomol. Chem.,* **2014**, *12*, 438-445.

37. Kim, J. I.; Shin, I.-S.; Kim, H.; Lee, J.-K. *J. Am. Chem. Soc.*, **2005**, *127*, 1614-1615.

38. Lai, R. Y.; Bard, A. J. *J. Phys. Chem. A*, **2003**, *107,* 3335-3340.

이리듐 복합체를 이용한 전기화학적 발광 기반의 황화이온 프로브

황화 이온을 효과적으로 검출하기 위한 다양한 화학 센서의 개발이 이루어져 왔다. 그러나 기존의 방법들은 분석 과정이 복잡하고 부피가 큰 측정 장비가 필요하기 때문에 임상 응용되기에 어려움이 있었다.

전기화학적 발광을 기반으로 한 화학 센서는 기존의 분석 방법들에 비해 감도가 높고 배경 신호가 없으며 검출 장비가 간단하다는 장점들이 있다. 이러한 특징들을 바탕으로, 전기화학발광 센서는 간편하게 임상 진단을 할 수 있는 현장 진단 장비로 개발될 수 있다.

우리는 고리형 이리듐 착물을 기반으로 하여, 황화 이온을 검출하기 위한 두 개의 전기화학적 발광 화학 센서 (1, 2)를 개발하였다. 다이나이트로페닐기를 광유발 전자 전달 소광체이자 황화 이온과의 반응 자리로써 이리듐 착물에 도입하였다. 다이나이트로페닐기는 황화 이온과 친핵성 고리 치환 반응을 하여 이리듐 착물로부터 분리되고 그에 따른 인광과 전기화학적 발광의 증가를 유도하였다. 탐지체 1 과 2 의 전기화학적 발광은 0–8

당량의 황화 이온 존재 하에 선형 상관관계를 보였다. 그리고 두 탐지체 모두 상당히 낮은 검출 한계를 보여주었다. 또한, 탐지체 1 과 2 는 다른 음이온들이나 바이오티올과는 반응하지 않고, 오직 황화 이온과 선택적으로 반응하여 전기화학발광을 크게 증가시켰다.